

Water Resources Research

RESEARCH ARTICLE

10.1029/2018WR023877

Key Points:

- The width, length, and surface area of the wetted stream channel varies with runoff as a power-law
- Total stream surface area increases with runoff by lateral and longitudinal expansion, which contribute equally to surface area expansion
- Nonperennial first-order streams present consistent stream width distributions when flowing

Correspondence to:

E. Barefoot,
eric.barefoot@rice.edu

Citation:

Barefoot, E., Pavelsky, T. M., Allen, G. H., Zimmer, M. A., & McGlynn, B. L. (2019). Temporally variable stream width and surface area distributions in a headwater catchment. *Water Resources Research*, 55, 7166–7181. <https://doi.org/10.1029/2018WR023877>


Received 9 AUG 2018

Accepted 24 JUL 2019

Accepted article online 30 JUL 2019

Published online 23 AUG 2019

Temporally Variable Stream Width and Surface Area Distributions in a Headwater Catchment

Eric Barefoot^{1,2} , Tamlin M. Pavelsky¹ , George H. Allen^{1,3} , Margaret A. Zimmer⁴ , and Brian L. McGlynn⁵ 

¹Department of Geological Sciences, The University of North Carolina, Chapel Hill, NC, USA, ²Now at Department of Earth, Environmental, and Planetary Sciences, Rice University, Houston, TX, USA, ³Now at Department of Geography, Texas A&M University, College Station, TX, USA, ⁴Earth and Planetary Sciences Department, The University of California, Santa Cruz, CA, USA, ⁵Nicholas School of the Environment, Duke University, Durham, NC, USA

Abstract Headwater stream networks expand and contract in response to event-driven and seasonal catchment wetness conditions. This dynamic behavior drives variability in the width, length, and surface area of streams, important parameters for constraining a range of ecological and biogeochemical processes, such as atmospheric gas exchange. While the longitudinal expansion and contraction of streams has been studied for some time, variability in stream widths remains poorly understood. Recent studies have found that stream widths at average baseflow conditions follow a log-normal frequency distribution across diverse physiographies. To examine how the distribution of widths varies with flow conditions, we surveyed stream widths 12 times across a 48.4-ha research watershed, located in the Duke Forest in central North Carolina, USA. Here, we show that as runoff increased from the 37th to 99th percentiles of flow, flowing streams widened across the network (“lateral expansion”) and streamflow simultaneously extended upstream to reactivate dry channels (“longitudinal expansion”). In general, as runoff increased, the marginal increase in stream surface area was equally divided between longitudinal and lateral expansion. Even so, the median stream width widens on average with increasing runoff, suggesting that longitudinal and lateral expansion affect the distribution of stream width differently. We find that the form of the relationship between stream width and runoff is a power law, which can be used to refine models for surface area estimation.

1. Introduction

Headwater streams are a vital component of the hydrosphere and a critical natural resource. Due to high rates of hyporheic exchange and tight coupling of aquatic and terrestrial ecosystems, biogeochemical cycling is rapid in small streams (Hill et al., 2010; Raymond et al., 2013). For example, gas exchange across the air/water interface in small headwater streams produces a net carbon dioxide (CO₂) flux from groundwater reservoirs to the atmosphere (Butman & Raymond, 2011; Raymond et al., 2013). This net flux of CO₂ is in part controlled by the surface area of the air/water interface (“stream surface area”), which is computed as the product of stream width and the active drainage network (ADN) length (Butman & Raymond, 2011). Stream width and length, therefore, are important parameters for estimating CO₂ efflux from streams. Moreover, stream width is a core parameter for modeling a diverse suite of processes such as groundwater flow, hyporheic exchange, stream power, and sediment transport (Allen et al., 2013; Bencala et al., 2011; Gleason et al., 2014).

In large-scale perennial river networks, the ADN and the geomorphic channel network are generally considered to be equivalent. Based on this principle, studies applying hydromorphology to evaluate hydrological and biogeochemical processes along a river system rely on downstream hydraulic geometry scaling relationships, originally developed for larger rivers (Leopold & Maddock, 1953). These relationships assert that stream geometries vary as power-law functions, changing nonlinearly in scale and frequency with distance upstream from the river mouth. This class of relationships predicts that there are many narrow headwater streams, and relatively few large rivers. Indeed, at the scale of continents, river widths do appear to be distributed according to a power-law or Pareto distribution, consistent with a power-law scaling scheme (Allen & Pavelsky, 2018; Downing et al., 2012; Raymond et al., 2013).

However, power-law scaling has been found to be inappropriate for small streams (Anderson et al., 2004). At the smallest scales, the distinction between the ADN of flowing surface water and the geomorphic channel

network that contains it becomes important. Applying a power-law framework at the headwater scale implies that stream width will decrease monotonically upstream until streams are infinitesimally narrow, a prediction known to be untrue.

To solve this problem, a lower bound must be specified for the width of streams. Under a power-law scaling framework, a common approach predicts channel head locations using a critical drainage area criterion derived from digital elevation models (Montgomery & Dietrich, 1992; Tarboton et al., 1991). From this, we can estimate the maximum longitudinal extent of the ADN for streams and rivers, and a static minimum width is assumed for first order streams (e.g. Allen & Pavelsky, 2015). However, under power-law scaling, the abundance of streams increases while width decreases nonlinearly upstream. As a result, small deviations in the imposed lower bound have a large impact on estimates of stream surface area, and by extension, any biogeochemical fluxes or transport estimates derived from these.

Recent work has demonstrated that at the scale of a first-order watershed, the stream width of the ADN at baseflow is distributed log-normally rather than as a Pareto distribution (Allen et al., 2018). The characteristics of the stream width distribution appear to be consistent across different lithologies, climates, and land use regimes, extending prior work on single river reaches to headwater networks (Moody & Troutman, 2002). In contrast to power-law scaling, where the lower bound for the width of first order channels is arbitrary, a log-normal distribution allows a most common, or modal, stream width. The most common stream width is a natural lower bound that may be consistent across different environments (Allen et al., 2018), extending stream network width scaling relationships.

However, the framework from Allen et al. (2018) primarily considers stream width distributions under average baseflow conditions. Little consideration to date has been given to assessing how stream width distributions of the ADN change temporally in the same headwater catchment across a range of runoff conditions. Characterizing this variation is the focus of our study, in which we examine changes to the parameters that describe a log-normal distribution fitted to stream width data. We cast our analysis in terms of changes to the location (μ) and shape (σ) parameters of the log-normal distribution with runoff. Respectively, these are the mean and standard deviation of the log-transformed stream widths. These metrics are chosen because they are independent of catchment scale and describe how stream width varies throughout the catchment.

We hypothesize that changes in μ and σ of the width distributions are driven by two factors, both increasing with runoff: (1) *longitudinal* lengthening of the ADN and (2) *lateral* widening of already flowing streams. Small headwater networks expand longitudinally in response to increased runoff (Blyth & Rodda, 1973; Day, 1978; Godsey & Kirchner, 2014; Gregory & Walling, 1968). On average, lower-order stream segments are narrower than higher-order streams (Leopold & Maddock, 1953). Therefore, with increased runoff, longitudinal expansion is expected to decrease μ by shifting the location of the width distribution to the left, and also decrease σ , narrowing the distribution (Figure 1, scenario C). In contrast, we hypothesize that lateral expansion due to increased runoff will increase μ and σ , thereby shifting the width distribution to the right (Figure 1, scenario B). A “balanced equilibrium” state would result if these two mechanisms interacted to stabilize the width distribution despite highly variable runoff. Thus, the final state of the system would remain buffered despite heterogeneous runoff generation processes as driven by stratified groundwater reservoirs, seasonal differences in evapotranspiration, and lateral variations in connectivity (Hewlett & Hibbert, 1967; Kosugi et al., 2006; Robinson et al., 1995).

Here, we quantify the temporal variability of stream width, test the relative impact of longitudinal and lateral network expansion on ADN stream width distributions, and examine their relative contributions to buffering stream width distribution parameters. We use 12 spatially dense surveys of stream width and length across a range of flow conditions at Stony Creek, a 48.4-ha headwater research catchment in the Duke Forest in the Piedmont region of North Carolina, USA.

2. Study Area

The Stony Creek Research Watershed is located within the Edeburn Division of the Duke Forest, North Carolina, USA (Figure 2). Underlain by low-grade metamorphic bedrock with granitic intrusions, the Stony Creek watershed has well-drained, silty loam soils characteristic of the Carolina Slate Belt in the Piedmont physiographic region (Boggs et al., 2013). The annual average drainage density is 4.89 km/km²,

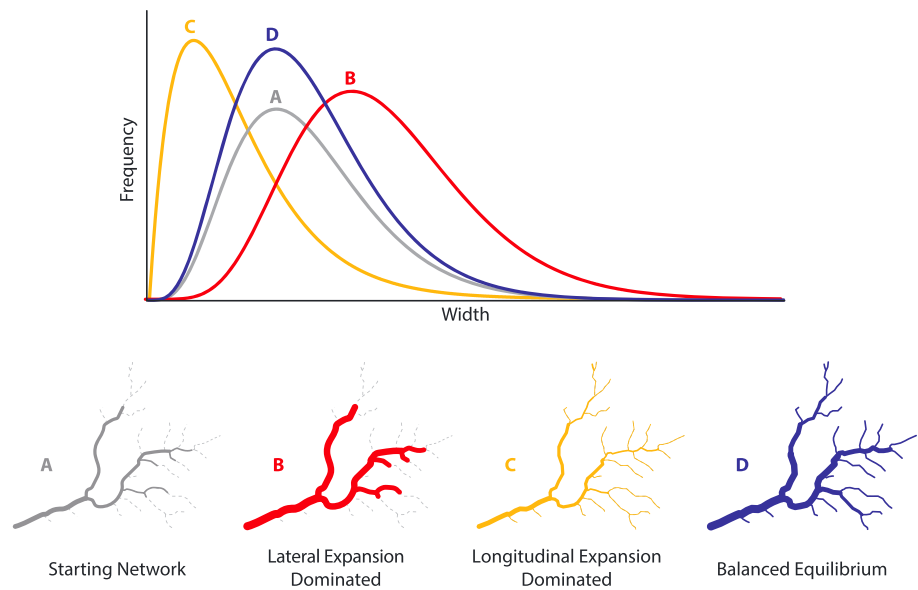


Figure 1. Starting from a hypothetical starting drainage network A, we propose three different possible scenarios of network expansion in response to increased runoff. Scenario B proposes that the active drainage network accommodates increased runoff mainly by widening at all points without appreciably extending into headwaters (lateral expansion). Scenario C assumes that the active drainage network simply extends into smaller headwaters without correspondingly increasing channel width everywhere (longitudinal expansion). Scenario D demonstrates the two mechanisms interacting to produce balanced equilibrium. The hypothesized width distributions for each scenario are shown above.

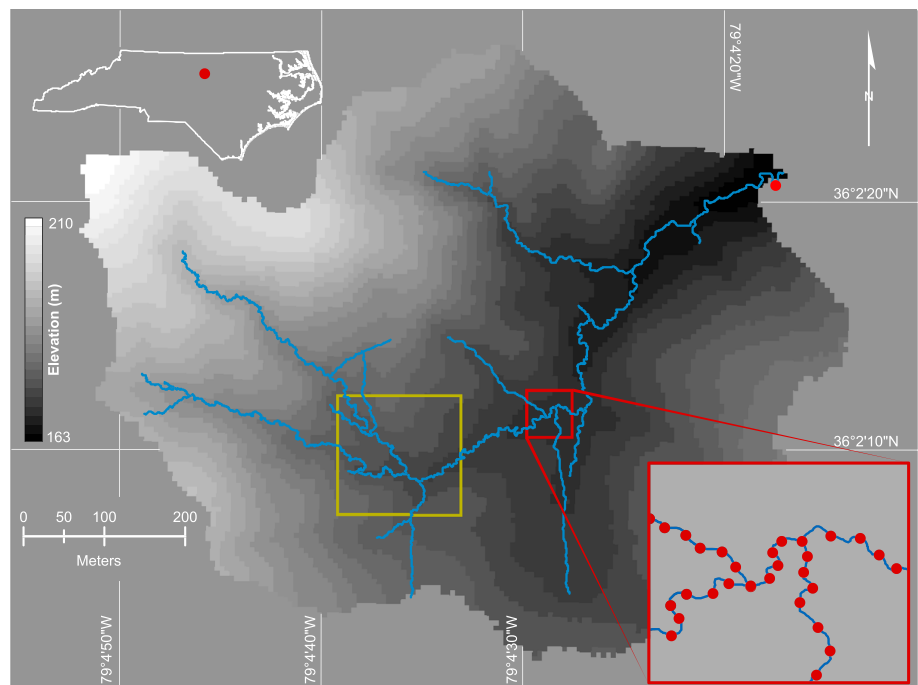


Figure 2. Map of study area showing location of all stream segments for the maximum observed active drainage network in blue. The red inset shows how we constructed our sampling network, with markers spaced every 5 m along the thalweg. Also shown in the red point is the location of the gauging station at the basin outlet. The yellow box shows the extent of the network shown in Figure 5. The location of the watershed in North Carolina, USA, is shown in the top left.

the average channel slope is 5.8%. Stony Creek has a humid subtropical climate, with relatively uniform monthly precipitation almost entirely composed of rain, and a long growing season (Kottek et al., 2006). Measured over the 2016 water year, precipitation was 1,376 mm, evapotranspiration was 720 mm, and runoff was 397 mm (Novick et al., 2016; Zimmer & McGlynn, 2018). Stony Creek has a stratified groundwater system, where tributaries are primarily fed by a shallow, flashy groundwater system. The mainstem is fed by a deeper, perennial groundwater system. The two systems are separated by impermeable soil horizons. Formerly cultivated as cropland, Stony Creek contains many relict anthropogenic structures, especially ditches and earthenworks, which have since become active stream channels. Since 1931, when the land was incorporated into Duke Forest, the site has been periodically harvested and burned for research and management purposes. It is predominantly forested, with loblolly pine (*Pinus taeda*), oak (*Quercus* spp.), sweetgum (*Liquidambar styraciflua*), and tulip poplar (*Liriodendron tulipifera*). See Zimmer and McGlynn (2017a, 2017b) for additional details on the hydrologic characteristics of Stony Creek.

3. Methods

We conducted 12 surveys of wetted stream widths from October 2015 to March 2016 at a range of runoff conditions (Table 1). We mapped the centerlines of the streams manually, guided by optical imagery from Google Earth and Global Positioning System (GPS) track data (Garmin Oregon 450t, 5-m horizontal accuracy). In densely vegetated areas, GPS tracks and imagery could not resolve the detailed planform geometry of the stream, so we corroborated our stream centerlines with field observations of stream segment length. We measured width at fixed measurement sites spaced at 5-m intervals throughout the wetted channel network at a range of stream runoff magnitudes to characterize stream width distributions as a function of stream surface area along the entire drainage network (740 sampling sites; Figure 2, red inset). We measured distance between measurement sites along the channel thalweg with a measuring tape and marked each site with a survey flag. For each survey, we measured the wetted width orthogonal to the stream thalweg at every marker flag with a standard tape measure.

We defined a stream as flowing water in a channel, including ephemeral channels formed in leaf litter (Allen et al., 2018). When a stream divided into multiple channels, we visually estimated the percentage of the stream that was dry to capture both the overall wetted width and a record of multithread channel behavior (Allen & Pavelsky, 2015). Multithreaded channel sites comprised approximately 7% of all measured data. When a sample location had no flowing water, a width of zero was recorded. Each survey contained 732–740 measurements and was completed in less than four hours to capture a temporal snapshot of the network. Occasionally, a sampling location marker was completely inundated, buried by sediment during a large event, or washed downstream. In such cases, we recorded the width as a missing value and replaced the lost marker flag before the next survey. These missing values comprise a small proportion (0.00 to 0.81%) of the total number of measurements in each survey. Measurement error was estimated by measuring a single-threaded reach of the stream five times across consistent runoff conditions. We found that the standard error for width was 3 cm.

For each survey, we paired width data with runoff measured at the watershed outlet. Stream stage was measured at a 5-min interval and converted to discharge based on a stage-streamflow rating curve constrained by 22 instantaneous discharge measurements collected over a wide range of flow conditions (Zimmer & McGlynn, 2017b). We then calculated mean runoff during each survey. Within a given survey, runoff varied by up to 218% and as little as 1.4% of mean flow. Most surveys had relatively low runoff variability, but two surveys taken during steeply rising and falling hydrographs had high runoff variation (see Table 1).

We conducted surveys at a wide range of runoff conditions spanning the 37th to 99th flow percentiles, estimated from discharge data from the nearest U.S. Geological Survey gauging station 12.7 km away on Bolin Creek (U.S. Geological Survey 0209734440), a record spanning 2012–2017. The Bolin Creek gauging station data were used to augment the relatively short record of runoff from Stony Creek itself. The lowest value of runoff (0.0002 mm/hr) was effectively zero at the gauge in Stony Creek, and therefore, this case was excluded from the analysis. The remaining surveys ranged by a factor of 17, from 0.055 to 0.953 mm/hr.

It is important to note that during periods of overbank flow, runoff is no longer confined to the channel, and changes in stream surface area will no longer be guided by channel morphology. Accordingly, we exclude one survey where there was substantial overbank flow (survey 3, see Table 1) from our analyses involving

Table 1
Summary Data for Each Survey at Stony Creek

Survey	Survey date	Runoff (mm/hr)	Flow percentile (%)	Range of runoff (mm/hr)	μ (ln cm)	σ (ln cm)	K-S test p -value
1	27 October 2015	0.056	37	0.0098	3.91	0.75	0.945
2	9 November 2015	0.410	98	0.8960	4.03	0.86	0.005
3	19 November 2015	0.953	99	1.3597	4.45	0.73	0.015
4	20 November 2015	0.203	91	0.0094	4.06	0.72	0.217
5	9 December 2015	0.108	47	0.0016	3.94	0.76	0.104
6	28 January 2016	0.216	89	0.0074	4.26	0.70	0.182
7	2 February 2016	0.114	68	0.0048	4.15	0.66	0.256
8	14 February 2016	0.065	57	0.0033	3.92	0.69	0.076
9	16 February 2016	0.419	98	0.1958	4.33	0.70	0.096
10	23 February 2016	0.674	92	0.3002	4.37	0.71	0.438
11	4 March 2016	0.104	69	0.0030	4.08	0.74	0.038
12	4 March 2016	0.106	69	0.0015	4.11	0.70	0.136

Survey	Mean width \pm SE (cm)	Mode width (cm)	Drainage density (km/km ²)	ADN length (m)	Flowing fraction of maximum ADN	Stream surface area (m ²)	Aspect ratio (L/w)
1	64 \pm 47	38	1.653	800	0.216	518	1,233
2	75 \pm 53	32	5.589	2,705	0.739	2,044	3,579
3	108 \pm 79	71	6.519	3,155	0.859	3,429	2,902
4	73 \pm 52	41	5.444	2,635	0.718	1,946	3,566
5	65 \pm 43	36	3.802	1,840	0.501	1,207	2,804
6	89 \pm 64	48	6.064	2,935	0.794	2,622	3,285
7	77 \pm 49	44	5.310	2,570	0.695	1,991	3,317
8	61 \pm 38	41	4.421	2,140	0.578	1,321	3,466
9	94 \pm 65	48	6.612	3,200	0.868	3,025	3,384
10	99 \pm 74	52	7.159	3,465	0.938	3,456	3,473
11	75 \pm 51	43	5.486	2,655	0.721	1,991	3,539
12	76 \pm 52	43	5.527	2,675	0.727	2,036	3,513

Note. Key hydrological variables are listed for each survey. Parameters defining the location (μ) and shape (σ) parameters of the lognormal distribution, along with the goodness-of-fit statistics for the Kolmogorov-Smirnov test. Mean width, mode width, and other geometric characteristics of the stream network are also listed.

predictive relationships. In effect, this event represents a different mechanism for stream surface area generation, and we lack sufficient data to constrain its functional form. However, this event reveals important details about how streams respond to extreme conditions, and it is included in other analyses as a comparison to more moderate flows.

To analyze trends in stream width distribution parameters across changing runoff conditions, we log-transformed stream width data and employed a linear mixed-effects statistical model to assess changes in μ as a power-law function of runoff (Bates et al., 2015). In this framework, μ is modeled with runoff as the fixed effect, and survey flag location is modeled as the random effect as both the intercept and slope on runoff (see Table 2). Model selection and evaluation were made on the basis of a comparison of the Akaike information criterion calculated for a suite of candidate models (Burnham & Anderson, 2002). All analysis was conducted using R software (R Core Team, 2018).

We assessed log-normal behavior by fitting a log-normal distribution to each width survey using maximum likelihood estimation (Venables & Ripley, 2002) and evaluated the goodness-of-fit to the log-normal distribution using a Kolmogorov-Smirnov test (Massey, 1951). The stream width frequency distributions were readily characterized by log-normal distributions (Kolmogorov-Smirnov $D = 0.053 \pm 0.011$, p -values = 0.20 ± 0.25). As such, the distributions are well parameterized by μ and σ , the mean, and standard deviation of the log-transformed data.

For each survey, we calculated the total stream surface area by summing all the stream widths, multiplied by the distance between survey points (5 m). Trends in surface area generation with increased runoff were analyzed using a fixed-effects model. To evaluate the relative magnitude of lateral versus longitudinal network

Table 2
Models Fitted to Estimate the Effect of Runoff on μ

Model	β_0	δ	β_1	γ	ϵ	AIC
$\mu = (\beta_0 + \delta) + \gamma \log R + \epsilon$	4.09 ± 0.02	0.84	–	0.36	0.36	7,113.4
$\mu = (\beta_0 + \delta) + (\beta_1 + \gamma) \log R + \epsilon$	4.50 ± 0.03	0.69	0.28 ± 0.01	0.21	0.36	6,714.8*
$\log A_s = \beta_0 + \beta_1 \log R + \epsilon$	7.92 ± 0.17	–	0.20 ± 0.06	–	0.41	–
$\mu = \beta_0 + \beta_1 P + \epsilon$	3.62 ± 0.19	–	0.006 ± 0.002	–	0.17	–
$\log L = \beta_0 + \beta_1 \log R + \epsilon$	8.02 ± 0.13	–	0.13 ± 0.05	–	0.33	–

Note. The first is a null model with random effects only on the slope and intercept on runoff. The second model is a mixed-effects model for a power law fit. The lower three models summarize trends in surface area, μ , and active drainage network length with runoff or flow percentile. These models were fit as fixed-effect models. AIC is used for model selection, with the preferred model and its associated AIC score indicated by an asterisk. δ , γ , and ϵ are reported as standard deviation of a random normal variate fitted in the model. Abbreviation: AIC, Akaike information criterion.

expansion effects on stream surface area generation, we compared a selection of paired surveys from the dataset and separated the total change in stream surface area from one survey to the next (A_T) into contributions from lateral and longitudinal expansion. Since we are only interested in the marginal increase in the area with a marginal increases in runoff, we ordered the surveys by runoff and only compared sequential pairs. We term A_{lon} the increase in stream surface area caused by the inundation of dry channels by longitudinal expansion and A_{lat} the change in area of already-wet locations by lateral expansion. We then compared the two effects for each pair of surveys and analyzed the width distributions of A_{lon} and A_{lat} . We also investigate the relationship of A_{lon} and A_{lat} to the marginal change in runoff.

4. Results

4.1. Network Expansion and Contraction, Fragmentation, and Width Variability

We observed substantial spatial and temporal variability of surface water expression in the Stony Creek watershed. Flowing stream width measurements across all surveys ranged from 2 to 831 cm (± 3 cm), and the length of the ADN ranged from 800 to 3465 m across a 0.055 to 0.953 mm/hr range of runoff (See Figure 3 and Table 1). Within individual surveys, stream width varied considerably along-network, with longitudinally adjacent sample locations differing by 28 cm on average and by as much as 620 cm. The

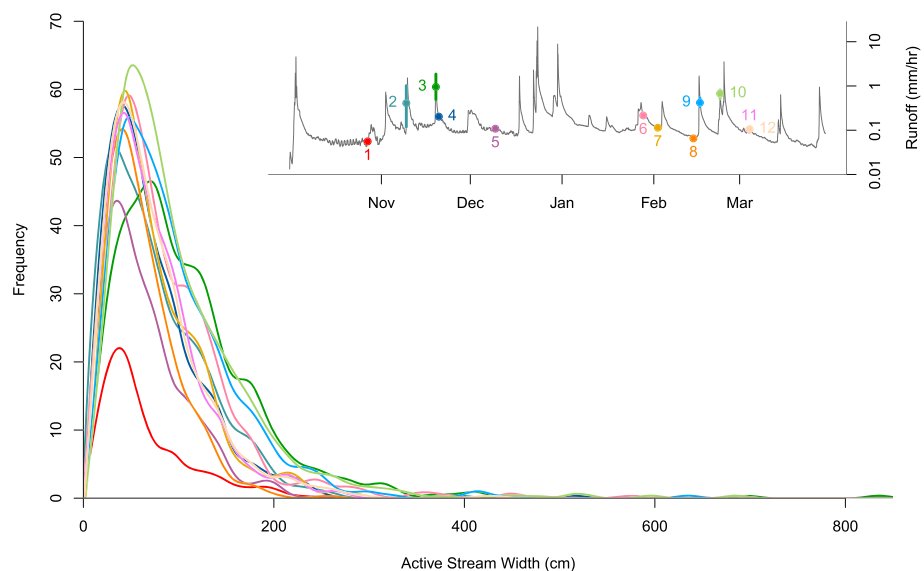


Figure 3. Width frequency distributions for each survey. A time series of streamflow at the watershed outlet is shown in the inset plot. Flows during each survey are represented by points, and if the range of flows during the survey period is larger than the point size, the range is represented by colored bars.

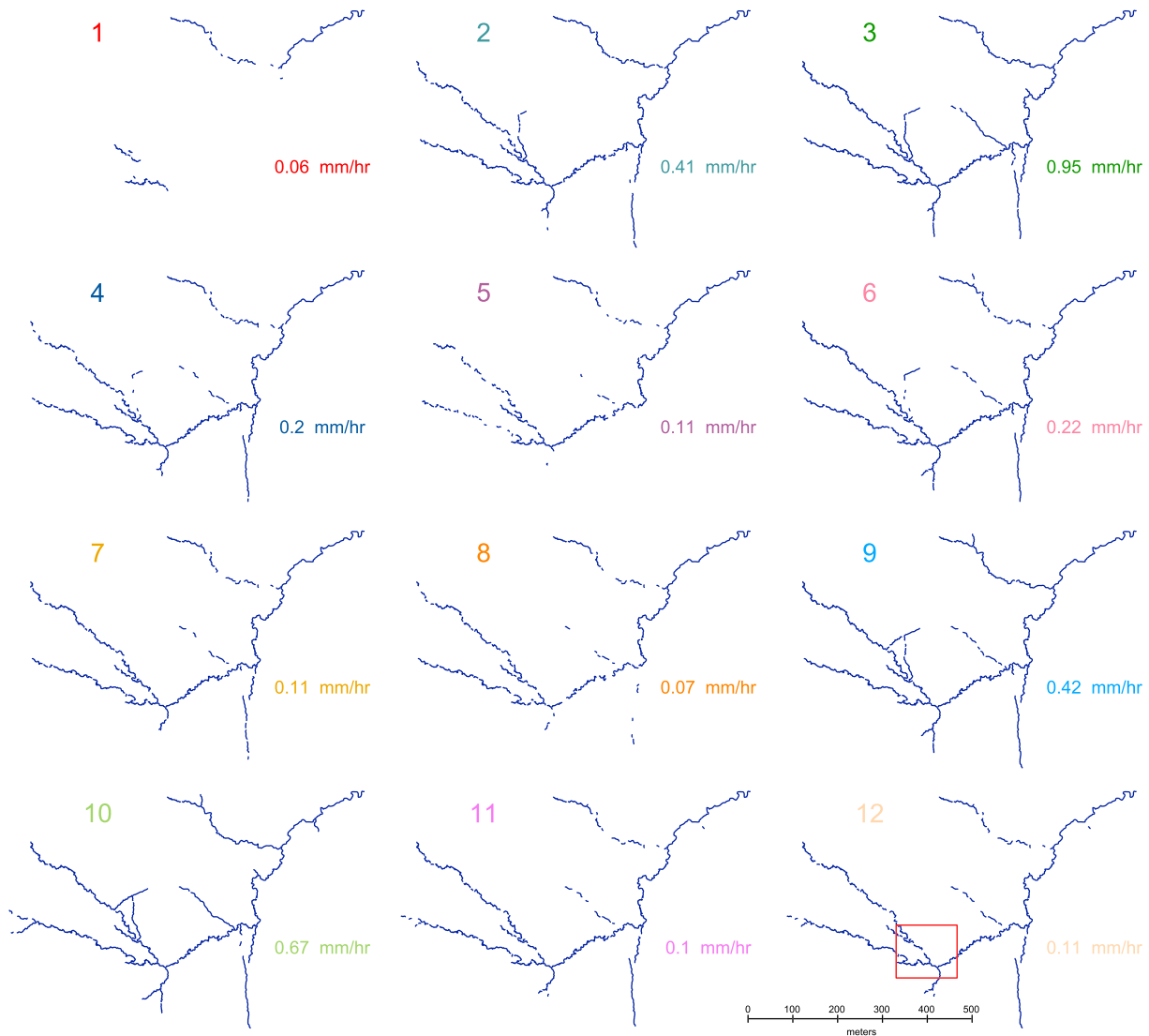


Figure 4. Variation in active drainage network connectivity across all surveys. Each panel represents a unique survey, and active streams are shown as blue lines. Network snapshots are ordered by survey date. The box in panel 12 shows the extent of Figure 5. Runoff at the outlet is shown for each survey in colored text. Variation in stream width across all surveys. This figure shows a subset of the basin to highlight fine-scale variations in width. The extent of this section is represented by the red box in panel 12 of figure. Each panel represents a snapshot ordered by survey date. Runoff at the outlet is shown for each survey in colored text.

flowing width of individual measurement locations was also highly variable through time. At some locations, stream width varied by up to 787 cm among all surveys, while at others it did not vary at all.

The Stony Creek ADN dynamically expanded and contracted as well as connected and disconnected in response to changing hydrologic conditions. Dynamic connectivity of flow between stream segments is a common phenomenon that has been observed in other studies across a broad range of landscapes and climates (Godsey & Kirchner, 2014; Jensen et al., 2019; Prancevic & Kirchner, 2019; Shaw, 2016; Whiting & Godsey, 2016; Zimmer et al., 2013). In general, first-order tributaries tended to disconnect from downstream segments and contract before higher order streams dried up, though this was not always the case. For example, Figure 4 shows the disappearance of large parts of the trunk stream in October (panel 1), while smaller tributaries remained flowing.

Stream widths across the catchment did not respond uniformly to changing runoff conditions. Some reaches like segment S07A were very sensitive to changing hydrologic conditions (see Figure 5). Others, like segment

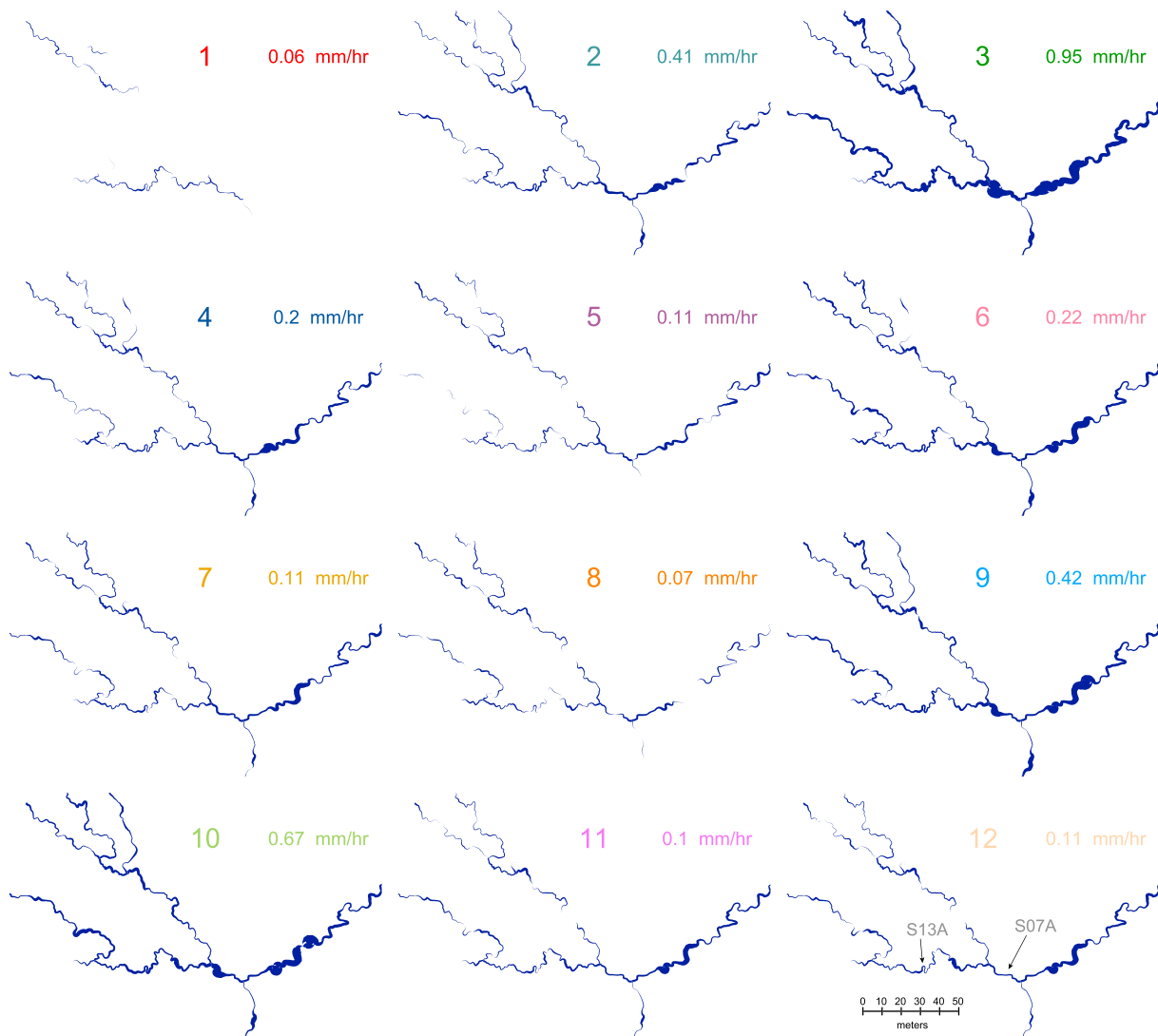


Figure 5. Variation in stream width across all surveys. This figure shows a subset of the basin to highlight fine-scale variations in width. The extent of this section is represented by the red box in panel 12 of figure. Each panel represents a snapshot ordered by survey date. Runoff at the outlet is shown for each survey in colored text.

S13A, were relatively insensitive. In fact, some reaches ceased flowing despite a catchment-wide increase in total stream surface area. We observed rare small-scale changes in channel morphology throughout the network, for instance, when logjams were cleared in large storm events or when trees fell and redirected stream flow. However, these changes to channel morphology were minor, and we do not expect them to have a significant impact on the results in this study.

4.2. Width and Area Distribution Kinematics

Width was found to vary systematically with runoff. In particular, μ covaried with runoff as a power law function. Because this study uses a repeat-measures design, the effect of runoff on μ was quantified using a mixed-effects model, where runoff was the fixed effect and the intercept and slope of width at each measurement point were both treated as random effects. Runoff effects were found to substantially improve the fit over a null model fit with random effects only, based on an Akaike information criterion difference of 398.6 (see Table 2). For this study, we consider moderate flows to be flows in excess of the 10th percentile but less than 90th percentile. Over the range of these flows, this effect translates to about a median of 25 cm

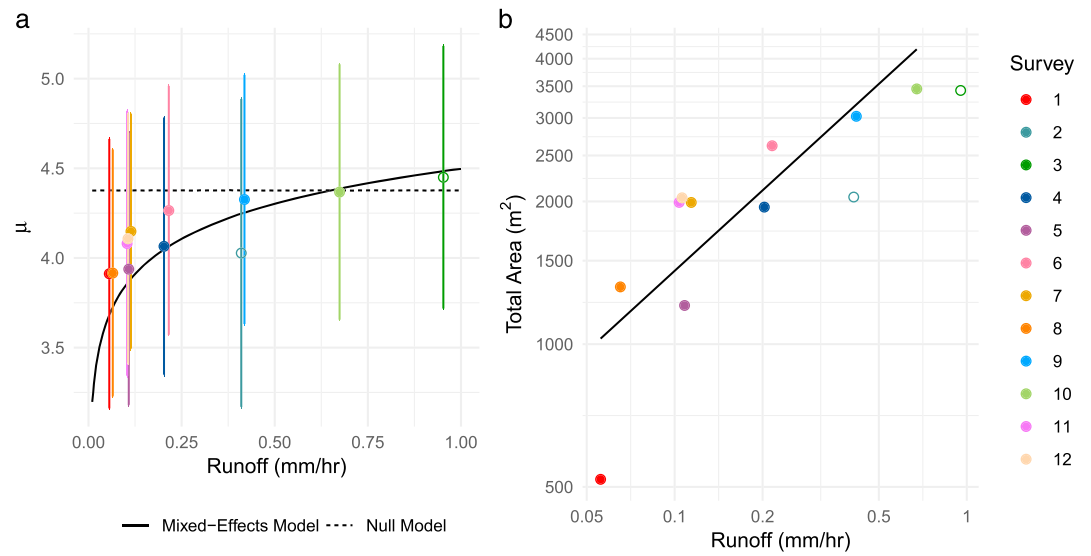


Figure 6. (a) Power-law relationship of μ with runoff at the outlet. The open circles were excluded from model for reasons described in sections 3 and 5.2. The model shown is a mixed-effects model, with random effects on sample location. Parameters and functional form are given in Table 2. A null model with only random effects is shown by the dashed line. (b) Power law relationship between total stream surface area and runoff as described by Equation (1).

of stream widening. The mean value of σ was estimated to be 0.711 ± 0.01 ln (cm); σ did not significantly covary with runoff ($F = 0.14$, $df = 11$, $p = 0.72$).

Total stream surface area (A_s , in m^2) ranged from 519 to 3,456 m^2 , which comprises 0.11 to 0.71% of the total catchment area, a value similar to recent global estimates via remote sensing (Allen & Pavelsky, 2015, 2018; Raymond et al., 2013). Total stream surface area also varied as a power-law function of runoff measured at the outlet (R , in mm/hr):

$$A_s = \alpha R^\beta \quad (1)$$

where $\beta = 0.197 \pm 0.06$ and $\alpha = 2738 \pm 1.2$ ($r^2 = 0.66$, p -value = 0.005, see Figure 6b and Table 2). Inundated stream surface area can be summarized as a rectangle with dimensions L and \bar{w} , where L is network length and \bar{w} is the mean width. Stream length varied with runoff as a power law, as observed in other studies (Godsey & Kirchner, 2014; Prancevic & Kirchner, 2019), while the relationship between length and width has not been investigated. We found that during moderate flows, the aspect ratio (L/\bar{w}) of the ADN was approximately constant.

To better understand the mechanisms by which surface area is added to streams with incremental increases in runoff, we compared the total change in stream surface area (ΔA_T) between eight pairs of surveys. Because we are interested in the relative contribution of longitudinal and lateral expansion with a marginal change in runoff, only pairs that are sequential when sorted by runoff are considered and changes in surface area are compared to the change in runoff between these pairs.

Figure 7 shows this process for a pair of example surveys (surveys 8 and 9). The total change in stream surface area calculated from pair-wise differences between the orange curve (survey 8) and the light blue (survey 9) in Figure 7a is the total stream surface area of newly inundated reaches plus the marginal increase in width at every point (ΔA_T) shown in Figure 7b. The width distribution for the pairwise differences can be separated into two distributions, one for A_{lon} , and one for A_{lat} , (Figure 7c). The integrated distribution for each effect represents the change in area. For this example, A_{lon} was 888 m^2 and A_{lat} was 810 m^2 . In this case, the ratio of the component for each effect to the total area change is close to 0.5 (0.52 and 0.47, respectively).

We tested whether the relative contributions of lateral and longitudinal expansion were consistently different from 0.5, the value that would be expected if both effects were in balance. Neither effect was found to be significantly different from 0.5 ($t = 1.11$, $df = 7$, $p = 0.31$). We then modeled the relative

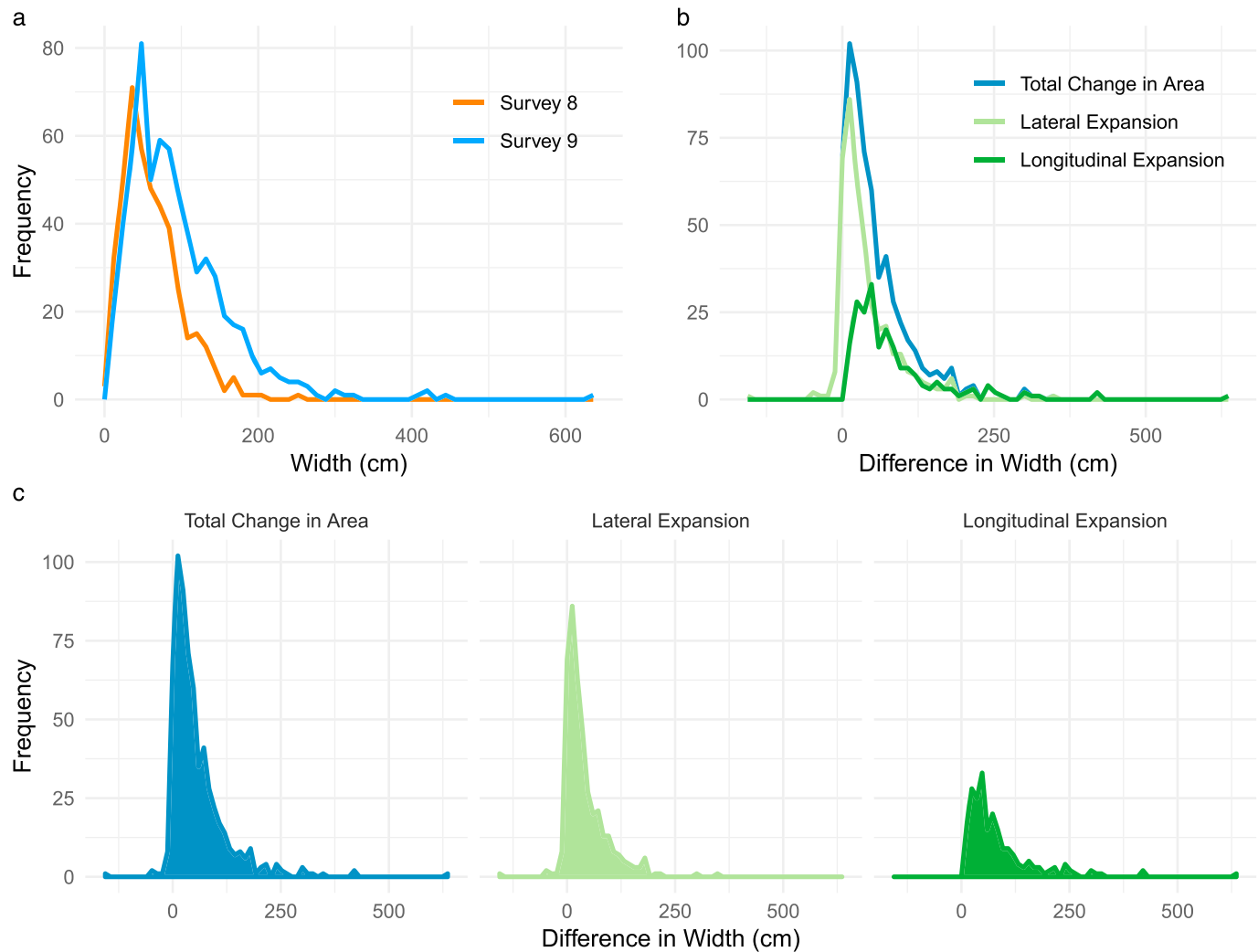


Figure 7. Demonstration of how stream surface area is added with a marginal increase in runoff. (a) An example pair of surveys, drawn in orange (survey 8 in Table 1) and light blue (survey 9), show changes in the distribution due to added surface area. (b) The difference in width at every location from survey 8 to survey 9 is plotted as the dark blue distribution. This distribution can be decomposed into two distributions, one encompassing lateral expansion (and in this case, some contraction) in width, and the other encompassing longitudinal expansion of the network. (c) The integrated differences in width comprise the change in surface area between the pair of surveys. In this way, we calculate ΔA_T , ΔA_{lat} , and ΔA_{lon} .

contribution of each expansion mechanism as a function of the marginal increase in runoff. Runoff was not found to be a significant effect ($F = 0.503$, $df = 1$, $p = 0.50$), suggesting that for every marginal increase in runoff, the additional surface area is approximately evenly divided between lateral and longitudinal expansion.

To better understand how stream width is distributed within and between the lateral and longitudinal components of stream expansion, we measured μ for the portion of the width distribution affected by each process for every pair of surveys. Again, using the example in Figure 7, the distribution for survey 9 can be decomposed into the portions affected by lateral and by longitudinal expansion. We found that as runoff increased, μ for segments affected by lateral expansion increased linearly with a slope of 0.98 ± 0.36 , (Figure 8a; $F = 7.24$, $df = 1$, $p = 0.036$), whereas the slope of μ with runoff for longitudinal expansion is not significantly different from zero (Figure 8a; $F = 0.04$, $df = 1$, $p = 0.84$). This indicates that longitudinal and lateral expansion have different impacts on the combined μ of the distribution. This effect is summarized by the power-law relation between runoff and μ in Figure 6a and Table 2. We also found that μ increases linearly with flow percentile, shown in Figure b ($F = 6.4$, $df = 11$, $p = 0.03$). In other words, lateral expansion increases μ more with bigger changes in runoff, whereas the effect of longitudinal expansion does not change with additional runoff.

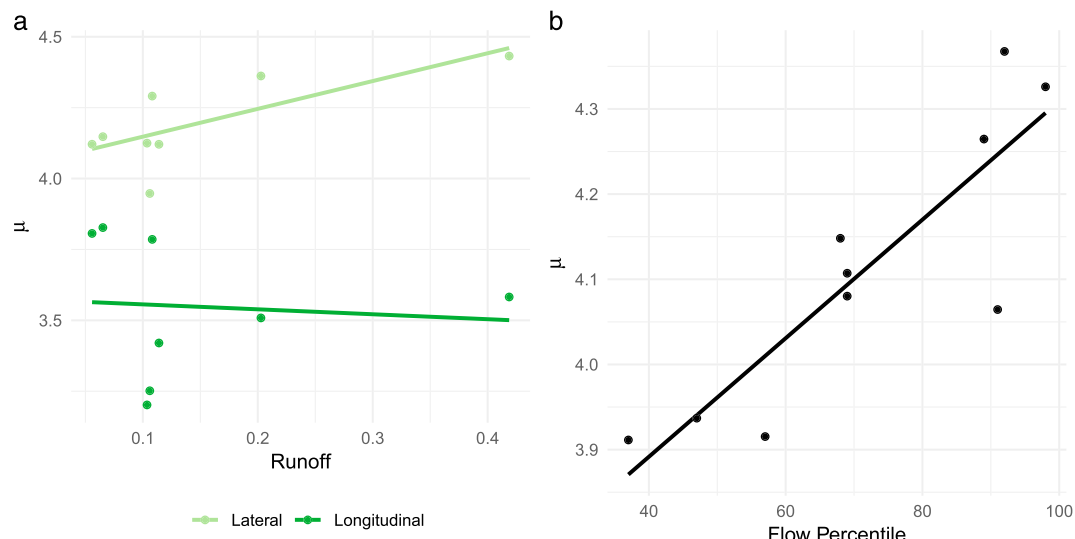


Figure 8. (a) Variation of μ for lateral and longitudinal components of stream expansion. Widths generated by lateral expansion systematically increases in μ with marginal increases in runoff. In contrast, μ for longitudinal expansion components is not significantly different from zero. (b) Flow percentile is a strong linear predictor of μ in the Stony Creek study catchment.

5. Discussion

In this study, we examined how the width and surface area of headwater streams changed across a range of runoff conditions. Our observations show that stream width is dynamic and that runoff is an important parameter for constraining the dimensions of stream surface area. We note that in our study site, both lateral and longitudinal expansion contribute equally to marginal increases in stream surface area and quantify how stream width is distributed and how it responds to changing flow conditions.

These components are the building blocks to construct a model for estimating stream surface area that accounts for both lengthening of the stream network and widening of individual streams. Better understanding the relationship between lateral and longitudinal expansion may provide insight into runoff generation processes (Beven & Wood, 1983). The dependence of width on runoff may also reflect topographic controls on streamflow generation (Prancevic & Kirchner, 2019). Evaluating the conceptual model posed above (Figure 1) in the context of our results will provide a basis for estimating stream surface area for many applications but also identify areas where streamflow generation knowledge can be more strongly developed.

5.1. Longitudinal and Lateral Expansion Contributions to Stream Surface Area

Figure 1 outlines the conceptual framework of our study. Three scenarios of changing surface area can arise from a baseline case (A), where the end-members are (B) dominance of lateral expansion, and (C) dominance of longitudinal expansion, while (D) balanced equilibrium represents an intermediate case. As hypothesized by Allen et al. (2018), we find that with increased runoff, streams simultaneously widen in place and extend upstream. In fact, we find that the magnitude of each of these two effects is, on average, equal. In other words, the addition of new water to the system produces an increase in the surface area of the streams, and on average 50% of this new surface area is due to lateral expansion and longitudinal expansion. This result implies that new surface area is not concentrated in either the trunk stream or the first order channels but is approximately evenly distributed, agreeing with a model of smoothly varying contributing area (Beven & Wood, 1983; Lee & Delleur, 1976).

Streamflow initiates when runoff exceeds the capacity for the subsurface to transmit flow (Godsey & Kirchner, 2014; Horton, 1945; Prancevic & Kirchner, 2019). Stream surface area for a given segment then increases with additional flux as a function of the channel shape (Dingman, 2007). Additional water, however, can be added to a flowing segment both through subsurface contributions, and from upstream channel flow (Robinson et al., 1995). Therefore, the response at one segment depends on both its contributing area and the network topology. Thus, the catchment-wide response of stream width should be related to the geomorphic unit hydrograph (Rodríguez-Iturbe & Valdés, 1979). The activation and saturation of different

storage elements in the catchment will change the topology of the stream network and, therefore, the resulting unit hydrograph. In this way, the changes in surface area observed at Stony Creek likely reflect dynamic source areas and corresponding feedback on the routing system (Beven & Wood, 1983).

Recent studies show that topography controls longitudinal expansion in many catchment systems, which have distinctive response curves for longitudinal network expansion with increasing runoff (Prancevic & Kirchner, 2019). These observations suggest that some streams may accommodate additional flow primarily through either lateral or longitudinal expansion, while Stony Creek represents an intermediate case where both expansion processes occur in tandem. Stony Creek has two distinct storage elements contributing to its runoff that are stratified vertically (Zimmer & McGlynn, 2017b). The shallow groundwater system has a flashier unit hydrograph, a shorter lag time, and preferentially feeds only a few subcatchments, whereas the deeper groundwater system preferentially supplies the main stem (Zimmer & McGlynn, 2018). The network at Stony Creek could therefore be expected a priori to have different surface area scaling when one groundwater storage system is active versus when both are active. The majority of our surveys span the time when both systems were active, so with the exception of very dry conditions such as survey 1, we can approximate the catchment system as having a single groundwater system made of many small storage elements and a dynamic source area.

While these catchment characteristics of Stony Creek could be the origin of its intermediate balance between lateral and longitudinal expansion, more work is needed to assess and extend this conceptual framework in other headwater systems, especially other geologic, tectonic, and climatic regimes. A balanced state where lateral and longitudinal expansion contribute equally to stream surface area could represent a preferred configuration toward which streams self-organize. If this is the case, balanced equilibrium of network expansion and contraction would be a generalizable result. For example, systems that rapidly expand longitudinally may have shallower groundwater systems and diminished subsurface transmission. In this case, we would expect a trade-off, where enhanced longitudinal expansion is matched by rapid lateral expansion in wide and shallow channels. Additional multitemporal width data in other catchments, however, would be required to assess the generalizability of the results shown here.

5.2. Stream Width Distributions Widen With Runoff

The equal contribution of lateral and longitudinal expansion to stream surface area would suggest that a balanced equilibrium prevails in the Stony Creek stream network, as shown in scenario D (Figure 1). However, across a range of moderate flow conditions in Stony Creek, the location parameter of the width distributions (μ) increased significantly with runoff (Figure 6a). The positive correlation of μ and runoff suggests that the lateral and longitudinal components of network expansion do not, in fact, hold the width distribution in a balanced equilibrium. Rather, this trend suggests that lateral expansion dominates over longitudinal expansion.

To resolve this apparent contradiction, we return to the assumption based on a power-law width scaling that longitudinal expansion generates streams that are narrower than the average (Leopold & Maddock, 1953). We hypothesized that as the ADN expands with increased runoff to occupy smaller channels, the new streams should be correspondingly narrower, a hypothesis our results show to be invalid. In fact, new streams generated by longitudinal expansion have a consistent width distribution, and a constant μ independent of runoff (Figure 8a). The constant μ value for longitudinal expansion is the same as the μ value for first order streams across all surveys.

In contrast, stream segments that were affected by lateral expansion and contraction with runoff are wider with every marginal increase in runoff (Figure 8a), as hypothesized. The total change in stream surface area is the sum of lateral and longitudinal components, so it follows that if each effect generates equivalent amounts of additional stream surface area, then μ of the resulting distribution will be a weighted average of μ for each of the two components. In this way, μ increases overall, since μ_{lat} increases while μ_{lon} is constant with runoff.

The power-law form of equation (1) predicting surface area as a function of runoff is similar to that observed for network length in other studies (e.g., Blyth & Rodda, 1973; Godsey & Kirchner, 2014; Prancevic & Kirchner, 2019). Since both the length and width of dynamic stream expansion scale as power laws, it is possible that insights into processes that affect stream length and surface area generation could be

complimentary. It is beyond the scope of this study to consider the topographic controls on stream width generation patterns but a larger study conducting multitemporal measurements of stream width across multiple catchments could shed light on this question. We expect that similar topographic controls may impact the morphology of channels (Prancevic & Kirchner, 2019) and therefore the local relationship between increased runoff and stream width. Catchment-wide patterns of topography could control the dependence of width on runoff in our model (β_1 ; Table 2) and therefore control patterns of stream surface area generation.

5.3. Applications to Estimating Stream Surface Area

Stream surface area is a primary parameter in calculations of stream gas efflux and biogeochemical cycling. Precisely estimating stream surface area is critical for constraining these processes. Previous approaches for estimating surface area (i.e., Allen et al., 2018) used mean survey values of μ and σ , regardless of flow conditions. Since these surveys spanned a range of flow conditions, using average values for μ and σ ($\mu = 3.47 \ln$ [cm] and $\sigma = 0.83 \ln$ [cm]) may appropriately approximate stream surface area at mean runoff, although more data are required to verify this assertion. The observed covariation between μ and runoff in Stony Creek presented here, however, suggests the need for a predictive relationship for stream surface area that incorporates runoff conditions. For cases in which the width distribution must be estimated for flow percentiles other than the mean, our data show that using a mean-only approach can lead to stream surface area estimation errors on the order of 30%. We propose a revision to the model proposed in Allen et al. (2018), where flow percentile is incorporated to adjust for changes in μ with runoff:

$$A_s = L \sum_1^N e^{\mu(P) + 0.83X} \quad (2)$$

where A_s is the surface area (m^2), X is a normally distributed random deviate such that $X \sim \mathcal{N}(0, 1)$, L is the ADN length (meters), N is the number of sampling points in the network, and $\mu(P)$ gives μ as a function of flow percentile (P), given here and with values for β_0 and β_1 in Table 2:

$$\mu = \beta_0 + \beta_1 P + \epsilon \quad (3)$$

Derived from the model fit shown in Figure 8b, this revision reduces the root-mean-squared error of the stream surface area estimate across all surveys examined here by approximately half. While this fit is based on data from Stony Creek only, the general behavior is expected to be generalizable to other catchments. Until additional data are collected in catchments of differing topography, it is unknown how the constants β_0 and β_1 will vary across catchments.

However, it is likely that these parameters will only vary across a narrow range. Allen et al. (2018) assert that the close clustering of observed μ values for physiographically diverse catchments represents a property of headwater catchments and channel systems, which is independent of runoff conditions. Our results confirm that μ values vary within a tight range but suggest that some of the unexplained variance in their data can be explained by variable runoff conditions. Because their surveys were conducted over a wide range of flow percentiles, some of the variability in μ across sites can be partitioned to a runoff term. However, the coefficients that determine the sensitivity of μ for every catchment, and their dependence on topography, remain unknown.

5.4. Additional Considerations for Stream Surface Area Prediction

The conceptual model for lateral and longitudinal expansion of the stream network described in Figure 1 does not hold under all circumstances. First, it is critical to recognize that this model does not hold during overbank flows. We observed one case of significant overbank flow (survey 3; see Table 1), which was also the highest magnitude runoff event surveyed. It produced a width distribution with a substantially greater variance and larger μ than all other surveys (Table 1). At bankfull conditions, because the ADN has already filled the geomorphic channel network, further expansion occurs outside the channels, where flow is unconfined. In this case, lateral expansion will always dominate over longitudinal expansion.

We sought to capture active stream network snapshots during a wide range of runoff conditions and thus conducted most surveys in non-baseflow conditions. The majority of these surveys occurred on the falling

limb of storm hydrographs. Only one survey was conducted during the rising limb of a storm event (survey 2), and along with survey 3, is an outlier from the runoff-area curve (Figure 6b). This survey has a lower stream surface area than we would predict based on its runoff, and we hypothesize that there may be a hysteretic relationship between width distribution characteristics and runoff magnitude. Hysteretic relationships in shallow groundwater systems have been documented, and they have been shown to have impacts on the drainage density of the ADN (Day, 1978; Jensen et al., 2019; Zimmer & McGlynn, 2017b). The rapid activation of, and contributions from, a potentially perched shallow groundwater system during the rising limb of storm hydrographs, may drive this hysteretic behavior in Stony Creek. However, more data on the rising limbs of storm hydrographs are required to evaluate this hypothesis, but given the short timescales of rising limbs in most headwaters catchments, collection of this type of data is challenging.

The spatial and temporal distribution of stream surface area may give information about the dynamics of expansion and contraction of contributing source area and hydrological connectivity, critical for understanding watershed hydrology (Beven & Wood, 1983; Lee & Delleur, 1976). Until very recently, much of the process-based understanding of ADN expansion and contraction has focused singularly on the longitudinal dimension of surface drainage networks. Many studies have focused on the length of the ADN in response to changing runoff (Day, 1978; Godsey & Kirchner, 2014; Lee & Delleur, 1976; Prancevic & Kirchner, 2019), but relatively little is known about how temporally variable stream width contributes to patterns of surface area generation. Drainage networks have complex interactions with groundwater, and Zimmer and McGlynn (2017b, 2018) show that during precipitation events, longitudinal expansion in Stony Creek is often driven by shallow groundwater flow transported along high-transmissivity soil horizons. This finding agrees well with existing theory and research, where the expansion of the source area controls the distribution of flowing water (Beven & Wood, 1983). However, the interaction between dynamic source area and the geomorphic channel network, which drives lateral expansion of streams, remains poorly understood.

Stream surface area is also a critical parameter problems involving biogeochemical cycles that are tightly coupled to stream surface area, such as gaseous efflux from headwater streams (Butman & Raymond, 2011; Johnson et al., 2008; Zappa et al., 2007). Our observations suggest that while the spatiotemporal distribution of surface area in headwater streams is highly variable, the relative change in stream surface area due to lateral and longitudinal expansion is approximately equivalent across most flow conditions. Because stream surface area expands in such a way that it is not concentrated in any particular location in the network topology, local variability in stream surface area is unlikely to have a large impact on the average dissolved gas efflux. Therefore, the impact of surface area variation on CO₂ efflux across a range of runoff conditions can be approximated simply by estimating the total stream surface area. In the context of work by Raymond et al. (2013), Butman and Raymond (2011), Allen and Pavelsky (2018), and Allen et al. (2018), these results can aid in constraining future estimates of global CO₂ efflux from rivers.

6. Conclusions

Our results reveal that active flowing stream width in Stony Creek was highly variable in space and time, due to the interaction between variable hydrologic conditions, heterogeneous runoff generation processes, and stream channel morphology. Across flow conditions at our field site, we found that stream widths followed a log-normal distribution, characterized by a location (μ) and shape (σ) parameter. The location (μ) of the width distributions increased as a power-law function of runoff (Table 2), whereas the shape (σ) parameter of the width distribution did not change with runoff.

Streams simultaneously expanded laterally and longitudinally with increased runoff, and we observed that increases in stream surface area were equally partitioned between lateral and longitudinal ADN expansion in Stony Creek. Even so, we found that μ increased slightly with runoff because the aspect ratio of marginal increases in surface area was not the same for the two processes. Stream area generated by lateral expansion was characterized by wider streams with each marginal increase in runoff, whereas reactivated dry streams retained the same distribution parameters as first order streams with increased runoff.

We also observed a power law scaling relationship between stream surface area and runoff. We used this relationship to evaluate and refine a surface area model proposed by Allen et al. (2018), and we extended it to account for changes in flow conditions using an empirical fit between μ and flow percentile. This

refined model applies for moderate (10th–90th percentile) flow conditions. At conditions above bankfull discharge and during very dry conditions, we expect the equilibrium between lateral and longitudinal expansion to be disturbed. Longitudinal expansion is dominant at times when the network is dry, and lateral expansion dominates when the catchment has completely filled the geomorphic channel network.

This work contributes to a growing body of evidence documenting the kinematics of drainage network expansion and contraction as well as fragmentation in headwater systems (e.g., Blyth & Rodda, 1973; Day, 1978; Godsey & Kirchner, 2014; Zimmer & McGlynn, 2018). However, many questions remain unanswered. For example, it is not known how topography controls stream widening, and generation of surface area. Future research should investigate these relationships, as they will be critical for predicting surface area generation patterns across sites and flow conditions.

Future research in this area should also investigate other hydraulic parameters such as flow velocity and depth. If these parameters also follow log-normal distributions, predictive relationships could be designed to extend standard downstream hydraulic geometry concepts to headwaters in a probabilistic framework. Such relationships could provide more robust models for streamflow that span scales. In addition, the potential presence of a hysteretic relationship in stream surface area through storm events could provide insight into event-driven runoff generation processes. If stream surface area is added preferentially on the falling limbs of event hydrographs, implications exist for the timing of biogeochemical cycling across the catchment due to event flow.

Parameters like the total stream surface area, which describe dynamic stream behavior, are critical for modeling and estimating a large number of hydrological processes, including sediment transport, hyporheic exchange, and atmospheric gas exchange. Small stream systems are the roots of the river network and ultimately have large impacts on the ecology, biogeochemistry, and hydrology of the entire river system. Understanding fine-scale hydromorphology and how it varies through time is an important component for describing and predicting processes across scales.

Data Availability

Data collected for this project and software used for analysis are available in a Zenodo online repository at <https://doi.org/10.5281/zenodo.1402808>

Acknowledgments

This research was in part supported by the Morehead-Cain Foundation and by NASA New Investigator Program Grant NNX12AD05G. Many thanks to Alex Brooks, Harley Burton, Michelle Gavel, Madelyn Percy, and Arik Tashie who all assisted with fieldwork. Work was performed in the Duke Forest Teaching and Research Laboratory. GIS data were provided by the Office of the Duke Forest at Duke University. The authors thank Tom E. X. Miller at Rice University for helpful advice on statistical modeling. E. B. in particular thanks Jeff Nittrouer for his support while completing this project. We additionally thank four reviewers who provided valuable feedback which significantly improved the quality of this manuscript. The authors declare no financial or other conflicts of interest.

References

- Allen, G. H., Barnes, J. B., Pavelsky, T. M., & Kirby, E. (2013). Lithologic and tectonic controls on bedrock channel form at the northwest Himalayan front. *Journal of Geophysical Research: Earth Surface*, *118*, 1806–1825. <https://doi.org/10.1002/jgrf.20113>
- Allen, G. H., & Pavelsky, T. M. (2015). Patterns of river width and surface area revealed by the satellite-derived North American River Width set. *Geophysical Research Letters*, *42*, 395–402. <https://doi.org/10.1002/2014GL062764>
- Allen, G. H., & Pavelsky, T. M. (2018). Global extent of rivers and streams. *Science*, eaat0636.
- Allen, G. H., Pavelsky, T. M., Barefoot, E. A., Lamb, M. P., Butman, D., Tashie, A., & Gleason, C. J. (2018). Similarity of stream width distributions across headwater systems. *Nature Communications*, *9*(1), 610. <https://doi.org/10.1038/s41467-018-02991-w>
- Anderson, R. J., Bledsoe, B. P., & Hession, W. C. (2004). Width of streams and rivers in response to vegetation bank material and other factors. Retrieved from <http://onlinelibrary.wiley.com/doi/10.1111/j.1752-1688.2004.tb01576.x/abstract>
- Bates, D., Mächler, M., Bolker, B., & Walker, S. (2015). Fitting linear mixed-effects models using lme4. *Journal of Statistical Software*, *67*(1), 1–48. <https://doi.org/10.18637/jss.v067.i01>
- Bencala, K. E., Gooseff, M. N., & Kimball, B. A. (2011). Rethinking hyporheic flow and transient storage to advance understanding of stream-catchment connections. *Water Resources Research*, *47*, W00H03. <https://doi.org/10.1029/2010WR010066>
- Beven, K., & Wood, E. F. (1983). Catchment geomorphology and the dynamics of runoff contributing areas. *Journal of Hydrology*, *65*(1–3), 139–158. [https://doi.org/10.1016/0022-1694\(83\)90214-7](https://doi.org/10.1016/0022-1694(83)90214-7)
- Blyth, K., & Rodda, J. C. (1973). A stream length study. *Water Resources Research*, *9*(5), 1454–1461. <https://doi.org/10.1029/WR009i005p01454>
- Boggs, J., Sun, G., Jones, D., & McNulty, S. G. (2013). Effect of soils on water quantity and quality in Piedmont Forested Headwater Watersheds of North Carolina. *JAWRA Journal of the American Water Resources Association*, *49*(1), 132–150. <https://doi.org/10.1111/jawr.12001>
- Burnham, K. P., & Anderson, D. R. (2002). *Model selection and multimodel inference: A practical information-theoretic approach* (2nd ed.). New York: Springer-Verlag. Retrieved from <https://www.springer.com/us/book/9780387953649>
- Butman, D., & Raymond, P. A. (2011). Significant efflux of carbon dioxide from streams and rivers in the United States. *Nature Geoscience*, *4*(12), 839–842. <https://doi.org/10.1038/ngeo1294>
- Day, D. G. (1978). Drainage density changes during rainfall. *Earth Surface Processes*, *3*(3), 319–326. <https://doi.org/10.1002/esp.3290030310>
- Dingman, L. (2007). Analytical derivation of at-a-station hydraulic–geometry relations. *Journal of Hydrology*, *334*(1–2), 17–27. <https://doi.org/10.1016/j.jhydrol.2006.09.021>
- Downing, J. A., Cole, J. J., Duarte, C. A., Middelburg, J. J., Melack, J. M., Prairie, Y. T., et al. (2012). Global abundance and size distribution of streams and rivers. *Inland Waters*, *2*(4), 229–236. <https://doi.org/10.5268/IW-2.4.502>

- Gleason, C. J., Smith, L. C., & Lee, J. (2014). Retrieval of river discharge solely from satellite imagery and at-many-stations hydraulic geometry: Sensitivity to river form and optimization parameters. *Water Resources Research*, *50*, 9604–9619. <https://doi.org/10.1002/2014WR016109>
- Godsey, S. E., & Kirchner, J. W. (2014). Dynamic, discontinuous stream networks: hydrologically driven variations in active drainage density, flowing channels and stream order. *Hydrological Processes*, *28*(23), 5791–5803. <https://doi.org/10.1002/hyp.10310>
- Gregory, K. J., & Walling, D. E. (1968). The variation of drainage density within a catchment. *Hydrological Sciences Journal*, *13*(2), 61–68.
- Hewlett, J. D., & Hibbert, A. R. (1967). Factors affecting the response of small watersheds to precipitation in humid areas. *Forest Hydrology*, *1*, 275–290.
- Hill, B. H., McCormick, F. H., Harvey, B. C., Johnson, S., Warren, M., & Elonen Colleen, M. (2010). Microbial enzyme activity, nutrient uptake and nutrient limitation in forested streams. *Freshwater Biology*, *55*(5), 1005–1019. <https://doi.org/10.1111/j.1365-2427.2009.02337.x>
- Horton, R. E. (1945). Erosional development of streams and their drainage basins; Hydrophysical approach to quantitative morphology. *Geological Society of America Bulletin*, *56*(3), 275–370. [https://doi.org/10.1130/0016-7606\(1945\)56\[275:EDOSAT\]2.0.CO;2](https://doi.org/10.1130/0016-7606(1945)56[275:EDOSAT]2.0.CO;2)
- Jensen, C. K., McGuire, K. J., McLaughlin, D. L., & Scott, D. T. (2019). Quantifying spatiotemporal variation in headwater stream length using flow intermittency sensors. *Environmental Monitoring and Assessment*, *191*(4), 226. <https://doi.org/10.1007/s10661-019-7373-8>
- Johnson, M. S., Lehmann, J., Riha, S. J., Krusche, A. V., Richey, J. E., Ometto, J. P. H. B., & Couto, E. G. (2008). CO₂ efflux from Amazonian headwater streams represents a significant fate for deep soil respiration. *Geophysical Research Letters*, *35*, L17401. <https://doi.org/10.1029/2008GL034619>
- Kosugi, K., Katsura, S., Katsuyama, M., & Mizuyama, T. (2006). Water flow processes in weathered granitic bedrock and their effects on runoff generation in a small headwater catchment. *Water Resources Research*, *42*, W02414. <https://doi.org/10.1029/2005WR004275>
- Kottek, M., Grieser, J., Beck, C., Rudolf, B., & Rubel, F. (2006). World map of the Köppen-Geiger climate classification updated. *Meteorologische Zeitschrift*, *15*(3), 259–263. <https://doi.org/10.1127/0941-2948/2006/0130>
- Lee, M. T., & Delleur, J. W. (1976). A variable source area model of the rainfall-runoff process based on the Watershed Stream Network. *Water Resources Research*, *12*(5), 1029–1036. <https://doi.org/10.1029/WR012i005p01029>
- Leopold, L. B., & Maddock, T. Jr. (1953). The hydraulic geometry of stream channels and some physiographic implications (USGS Numbered Series No. 252). Retrieved from. <http://pubs.er.usgs.gov/publication/pp252>
- Massey, F. J. (1951). The Kolmogorov-Smirnov Test for Goodness of Fit. *Journal of the American Statistical Association*, *46*(253), 68–78. <https://doi.org/10.2307/2280095>
- Montgomery, D. R., & Dietrich, W. E. (1992). Channel initiation and the problem of landscape scale. *Science*, *255*(5046), 826–830. <https://doi.org/10.1126/science.255.5046.826>
- Moody, J. A., & Troutman, B. M. (2002). Characterization of the spatial variability of channel morphology. *Earth Surface Processes and Landforms*, *27*(12), 1251–1266. <https://doi.org/10.1002/esp.403>
- Novick, K., Oishi, C., & Stoy, P. (2016). AmeriFlux US-Dk2 Duke Forest-hardwoods. <https://doi.org/10.17190/AMF/1246047>
- Prancevic, J. P., & Kirchner, J. W. (2019). Topographic controls on the extension and retraction of flowing streams. *Geophysical Research Letters*, *46*, 2084–2092. <https://doi.org/10.1029/2018GL081799>
- R Core Team (2018). *R: A language and environment for statistical computing*. Vienna, Austria. Retrieved from: R Foundation for Statistical Computing. <https://www.R-project.org/>
- Raymond, P. A., Hartmann, J., Lauerwald, R., Sobek, S., McDonald, C., Hoover, M., et al. (2013). Global carbon dioxide emissions from inland waters. *Nature*, *503*(7476), 355–359. <https://doi.org/10.1038/nature12760>
- Robinson, J. S., Sivapalan, M., & Snell, J. D. (1995). On the relative roles of hillslope processes, channel routing, and network geomorphology in the hydrologic response of natural catchments. *Water Resources Research*, *31*(12), 3089–3101. <https://doi.org/10.1029/95WR01948>
- Rodríguez-Iturbe, I., & Valdés, J. B. (1979). The geomorphologic structure of hydrologic response. *Water Resources Research*, *15*(6), 1409–1420. <https://doi.org/10.1029/WR015i006p01409>
- Shaw, S. B. (2016). Investigating the linkage between streamflow recession rates and channel network contraction in a mesoscale catchment in New York state: Linkage between recession rates and channel network contraction. *Hydrological Processes*, *30*(3), 479–492. <https://doi.org/10.1002/hyp.10626>
- Tarboton, D. G., Bras, R. L., & Rodríguez-Iturbe, I. (1991). On the extraction of channel networks from digital elevation data. *Hydrological Processes*, *5*(1), 81–100. <https://doi.org/10.1002/hyp.3360050107>
- Venables, W. N., & Ripley, B. D. (2002). Modern applied statistics with S. In *Statistics and computing* (4th ed., pp. 109–110). New York: Springer.
- Whiting, J. A., & Godsey, S. E. (2016). Discontinuous headwater stream networks with stable flowheads, Salmon River basin, Idaho. *Hydrological Processes*, *30*(13), 2305–2316. <https://doi.org/10.1002/hyp.10790>
- Zappa, C. J., McGillis, W. R., Raymond, P. A., Edson, J. B., Hints, E. J., Zemmellink, H. J., et al. (2007). Environmental turbulent mixing controls on air-water gas exchange in marine and aquatic systems. *Geophysical Research Letters*, *34*, L10601. <https://doi.org/10.1029/2006GL028790>
- Zimmer, M. A., Bailey, S. W., McGuire, K. J., & Bullen, T. D. (2013). Fine scale variations of surface water chemistry in an ephemeral to perennial drainage network. *Hydrological Processes*, *27*(24), 3438–3451. <https://doi.org/10.1002/hyp.9449>
- Zimmer, M. A., & McGlynn, B. L. (2017a). Bidirectional stream-groundwater flow in response to ephemeral and intermittent streamflow and groundwater seasonality. *Hydrological Processes*, *31*(22), 3871–3880. <https://doi.org/10.1002/hyp.11301>
- Zimmer, M. A., & McGlynn, B. L. (2017b). Ephemeral streamflow generation in a low relief, highly weathered catchment. *Water Resources Research*, *53*, 7055–7077. <https://doi.org/10.1002/2016WR019742>
- Zimmer, M. A., & McGlynn, B. L. (2018). Lateral, vertical, and longitudinal source area connectivity drive runoff and carbon export across watershed scales. *Water Resources Research*, *54*, 1576–1598. <https://doi.org/10.1002/2017WR021718>